Structural Chemistry (2020) 31:2463–2473
https://doi.org/10.1007/s11224-020-01600-1

ORIGINAL RESEARCH

Modeling the protein-nucleic acid base interactions through hydrogen-bonded complexes of N-heterocyclic analogs of Indene with amino acid side-chain mimics

Neha Chopra[1] · Geetanjali Chopra[1] · Damanjit Kaur[1]

Received: 15 April 2020 / Accepted: 22 July 2020 / Published online: 7 August 2020

Abstract

A series of hydrogen-bonded complexes between N-heterocyclic analogs of Indene and amino acid side-chain mimics have been analyzed employing second-order Møller-Plesset perturbation (MP2) theory and density functional theory with dispersion function (DFT-D) calculations with the aim of gaining greater insight in to the nature of intermolecular interactions in these systems. In this study, the hydrogen bonding ability of N-heterocyclic analogs of Indene towards amino acid side-chain mimics follows the sequence Azaindazole (AIND) > Indazole (IND) > Azaindole (AIN) > Indole (IN) whereas the hydrogen bonding ability of amino acid side-chain mimics towards N-heterocyclic analogs of Indene follows the sequence AcOH > $MeNH_2$ > MeOH > MeSH. Bader's theory of atoms in molecules (AIM) and natural bond orbitals (NBO) analyses are employed to elucidate the interaction characteristics in the complexes under study. The purpose of conducting these studies is to measure the relative strength of hydrogen bonding interactions such as N-H···O=C, N-H···O, N-H···S, N-H···N, and O-H···N in these complexes and their role in providing stability to the complexes. The AIM theory shows good correlation of the electron density and its Laplacian at the bond critical points (BCP) with the computed stabilization energy for all the complexes under study.

Keywords Hydrogen bonding · N-heterocyclic analogs of Indene · Amino acid side-chain mimics · NBO · AIM

Introduction

Hydrogen bonding is thought to play a critical role in stabilizing the structures of biological molecules such as proteins or nucleic acid [1, 2]. The participation of the amino acid in hydrogen bonding interaction is a well-recognized factor in many biologically relevant processes such as protein-nucleic acid interaction, protein-protein interaction, α-helices, and β-sheets formation. There are a number of amino acid residues that can form hydrogen bonds (HBs) via their side chains. Perhaps most notable of this category are side chains that contain hydroxyl (serine and threonine), acetic acid (aspartic and glutamic acids), amino (lysine and arginine), and thiol (cysteine) that are known to participate in HBs.

Among the molecules of biological interest, N-heterocyclic analogs of Indene (Indole, Indazole, Azaindole, Azaindazole) are structural constituents of many bioactive natural products and have gained much research pursuit in the field of medicinal chemistry. Such analogs of Indene are bicyclic heterocyclic compounds containing five-membered ring fused with six-membered ring. The hydrogen bonding interactions of N-heterocyclic analogs of Indene with amino acid side-chain mimics provide great opportunity for screening and discovery of diverse biologically active substances [3–14]. The choice of indole in the present study has been motivated as it is built in to proteins in the form of amino acid tryptophan, and its scaffold represents one of the most important structural subunits for the discovery of new drug candidates [15, 16]. Azaindole is another moiety of interest as it resembles molecules of the DNA base pair, and thus, is an important model system for the study of hydrogen bonding in DNA base pair. Indazole and Azaindazole moieties are important scaffolds which have attracted a considerable attention of medicinal chemists due to their pharmacological properties. The derivatives of

Electronic supplementary material The online version of this article (https://doi.org/10.1007/s11224-020-01600-1) contains supplementary material, which is available to authorized users.

✉ Neha Chopra
nehaomnamah@gmail.com

[1] Department of Chemistry, Guru Nanak Dev University, Amritsar 143005, India

Indazole and Azaindazole possess a variety of biological properties including anticancer, antibacterial, antiprotozoal, and anti-inflammatory activities [17–19].

The present study reports the hydrogen-bonded complexes in which the amino acid side-chain mimics are chosen as one partner and the N-heterocyclic analogs of Indene as another partner. The primary goal of the present study is to measure the relative strength of hydrogen bonding interactions such as N-H···O=C, N-H···O, N-H···S, N-H···N, O-H···N, S-H···N, and C-H···N in these complexes. Studying such interactions in these complexes is of great interest as their findings delineate the role of these HB interactions in the stability of protein-protein interfaces, protein-ligand complexes, protein-nucleic acid interactions, and DNA-drug complexes. It is worth noticing that the hydrogen bonding interaction N-H···S is ubiquitous in proteins [20–23] and its presence is manifested from the crystal structure data for β-lactam antibiotics such as penicillins, the active site of proteins like cytochrome-P450, and the iron-sulfur proteins [24, 25]. The study of structural, energetic, and topological parameters of this interaction will provide better insight into the understanding of the protein folding and biochemical reactions involving the formation and rupture of N-H···S HB.

Gas-phase quantum studies reveal that amino acid side-chain mimics coordinate to the N-heterocyclic analogs of Indene through N-H···O=C, N-H···O, N-H···S, and N-H···N hydrogen bonds which account for the significant changes in the structural, electronic, and energetic parameters of the Indene analogs. The results provided in this manuscript are helpful for experimental chemists working on protein structure or protein-nucleic acid-base interactions.

Results and discussions

Structural and energetic analysis

Hydrogen bonding interactions of N-heterocyclic analogs of Indene Indole (**IN**), Indazole (**IND**), Azaindole (**AIN**), and Azaindazole (**AIND**) (shown in Fig. 1) across the four amino acid side-chain mimics (**Z**), MeOH (mimic for serine and threonine), MeSH (mimic for cysteine), $MeNH_2$ (mimic for lysine), and AcOH (mimic for aspartic and glutamic acid), have been studied. A total of thirty-two complexes of the selected heterocyclic molecules with amino acid side-chain mimics have been optimized and their geometries are shown in Fig. 2. Indene comprises of six-membered and five-membered nitrogen-containing rings fused to one another. Indene **IN** has one potential site, N-H, incorporated in the five-membered ring that has a tendency to act either as a proton donor or simultaneously as a proton donor and acceptor, whereas in **IND**, there are two sites, N-H and N embedded in the five-membered ring. Relative to **IN** and **IND**, the corresponding aza compounds, **AIN** and **AIND**, have one additional proton acceptor site N incorporated in the six-membered ring. Both **AIN** and **AIND** exist in two positional isomers, **4AIN/AIND** and **7AIN/7AIND**, according to the position of nitrogen atom in the six-membered ring with respect to N-H of the five-membered ring. In our manuscript, we have labeled the pyridinic nitrogen of the five-membered ring in the N-heterocyclic analogs of Indene as "$\mathbf{N_5}$" and pyridinic nitrogen of the six-membered ring as "$\mathbf{N_6}$" for the sake of convenience. The potential HB donor/acceptor site associated with AcOH as well as MeOH is O-H while it is N-H for $MeNH_2$ and S-H for MeSH. AcOH also contains carbonyl oxygen as an additional HB acceptor site. Additionally, these amino acid side-chain mimics contain C-H that can also act as HB donor site towards the selected heterocyclics, forming C-H···N type interaction. The latter interaction serves as secondary interaction, offering additional stabilization to stronger HBs, and can perhaps further refinement to protein structure.

Hydrogen bonding interactions between N-heterocyclic analogs of Indene and amino acid side-chain mimics

(A) Indene-MeOH complexes The hydrogen-bonded complexes formed between Indene analogs and MeOH have been divided in to three categories, **I**, **II**, and **III**, on the basis of different HB donor and acceptor sites of both the units involved in hydrogen bonding interaction with each other (shown in Fig. 2). The complexes in which the N-H of Indene analogs acts simultaneously as the proton donor and acceptor towards the OH and methyl groups of MeOH respectively lead to the formation of the cyclic five-membered hydrogen-bonded ring labeled as "**I**." The second set of complexes designated as "**II**" exhibits cyclic six-membered hydrogen-bonded ring in which Indene analogs act as proton acceptor via its N_5 site and proton donor via its N-H site to the methyl group and OH site of MeOH. Another set of complexes is marked as "**III**" in which the OH site of MeOH acts as proton acceptor as well as donor towards N-H and N_5/N_6 sites of Indene analogs respectively, resulting the formation of five-membered ring in IND-MeOH **III** and 4AIND-MeOH **III** and six-membered ring in 7AIN-MeOH **III** and 7AIND-MeOH **III** complexes. The complexes 7AIN-MeOH **III** and 7AIND-MeOH **III** use N-H of five-membered ring and N_6 site of fused six-membered ring in hydrogen bonding with amino acid side-chain mimics whereas IND-MeOH **III** and 4AIND-MeOH **III** complexes utilize the N-H and N_5 site of five-membered ring of Indene analogs. The former complexes are more stable in comparison with the latter complexes as there is strong hydrogen bond network in the former complexes. This supports the fact that the N_6 site of the fused six-membered ring acts as a better HB acceptor in comparison with the N_5 site of the five-membered ring.

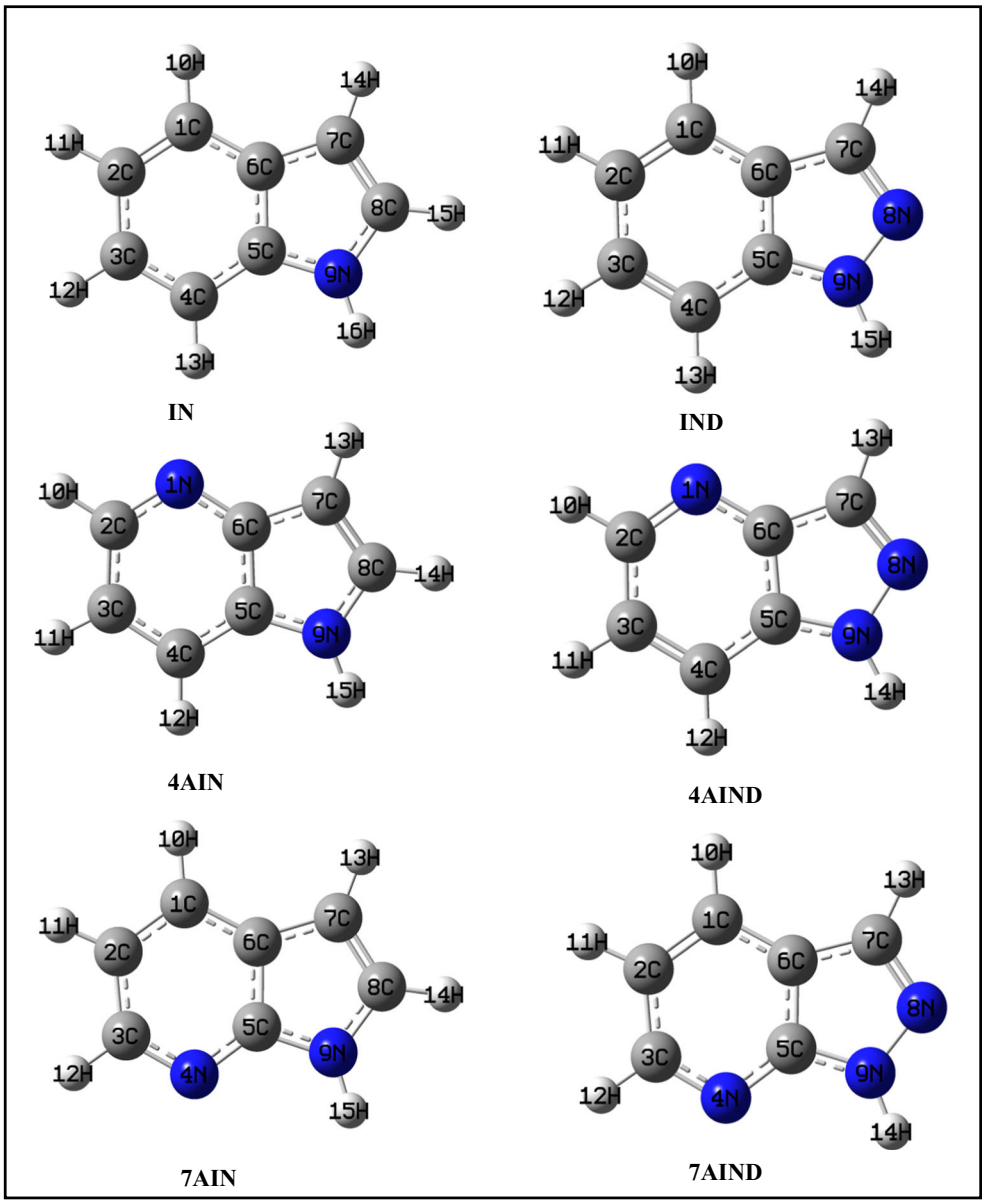

Fig. 1 Optimized geometries of N-heterocyclic analogs of Indene at MP2/aug-cc-pVDZ level

Out of these three sets, the third set is more stable in comparison with the first and second set of complexes as indicated by their stabilization energies. The most interesting aspect which has been observed is that the Indene-MeOH complexes have relatively higher stabilization energies in comparison with their corresponding Indene-H_2O complexes (shown in Table 1 and Table S1) as the additional methyl group induced the hydrogen bond switching, which can be ascribed to the electron donating property of the methyl group. This supports the assumption that additional carbon atom in the side-chain leads to significant changes in the drug-protein interactions and nucleobase-amino acid interactions.

(B) Indene-MeSH complexes MeSH binds to Indene analogs in three possible ways leading to the formation of three sets of complexes **IV**, **V**, and **VI**. The complexes in which Indene analogs bind to MeSH through single N-H···S HB are labeled as "**IV**." For "**V**" and "**VI**" set of complexes, it has been observed that MeSH exhibits exactly similar orientation to that of MeOH in **II** and **III** set of complexes, respectively. It is worth noticing that the replacement of oxygen with sulfur leads to longer HBs with subsequent weakening of N-H···S HBs, resulting in 1.12–3.88 kcal/mol lower stabilization energies of Indene-MeSH complexes relative to their corresponding Indene-MeOH complexes.

(C) Indene-$MeNH_2$ complexes $MeNH_2$ coordinates to Indene analogs in three ways turning out the formation of three sets of complexes labeled as "**VII**," "**VIII**," and "**IX**." The "**VII**" set of complexes involves monodentate HB formation with N-

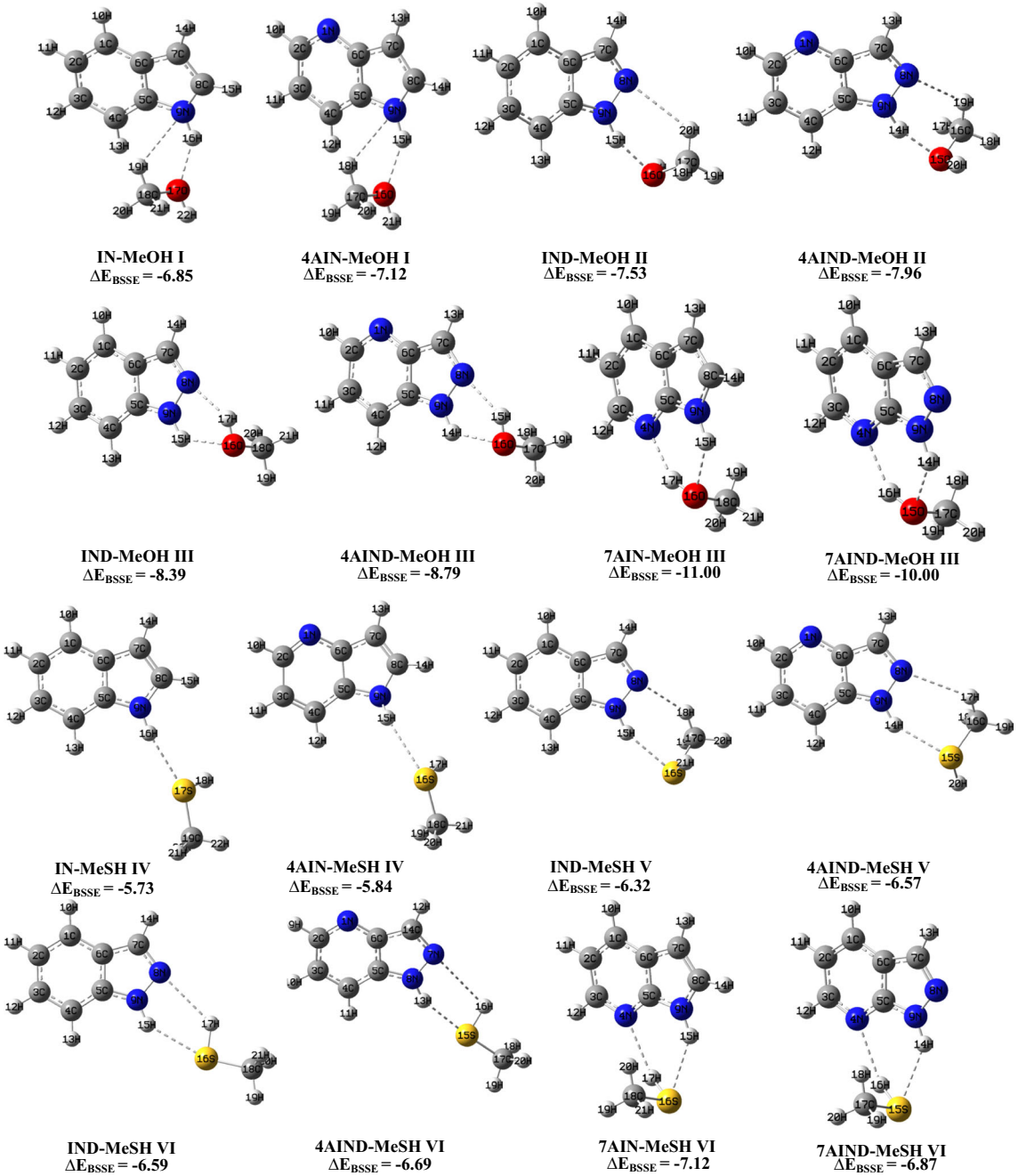

Fig. 2 Optimized geometries of 1:1 hydrogen-bonded complexes of N-heterocyclic analogs of Indene with amino acid side-chain mimics at MP2/aug-cc-pVDZ level

H···N interaction. In these complexes, N-H of Indene analogs hydrogen bond to "N" of $MeNH_2$ leading to the formation of the most linear HBs as depicted from HB angle values for IN-$MeNH_2$ **VII** (176.25°) and 4AIN-$MeNH_2$ **VII** (175.76°). The "**VIII**" set of complexes displays six-membered hydrogen-bonded ring structure, in which N-H and N_5 of Indene analogs act as proton donor and acceptor respectively towards nitrogen and methyl group of $MeNH_2$, leading to the formation of two HBs $_{Indene}$N-H···N and C-H···N_{Indene}. In these complexes, departure of N-H···N HB angle from the linearity is seen to be almost 20°. The "**IX**" set of complexes involves cyclic five-membered hydrogen-bonded ring structure in IND-$MeNH_2$ **IX** and 4AIND-$MeNH_2$ **IX** and six-membered hydrogen-bonded ring structure in 7AIN-$MeNH_2$ **IX** and 7AIND-$MeNH_2$ **IX** complexes. In these complexes, the amino group solely acts as the proton donor as well as proton acceptor to the N_5/N_6 and N-H sites of the Indene analogs, respectively, resulting in the formation of HBs $_{Indene}$N-H···N and N-H···N_{Indene}. Furthermore, the cyclic arrangement in these complexes results in more bent HBs; the deformation from the linearity lies in the range of 30° to 35° for $_{Indene}$N-H…N_{MeNH2} HB

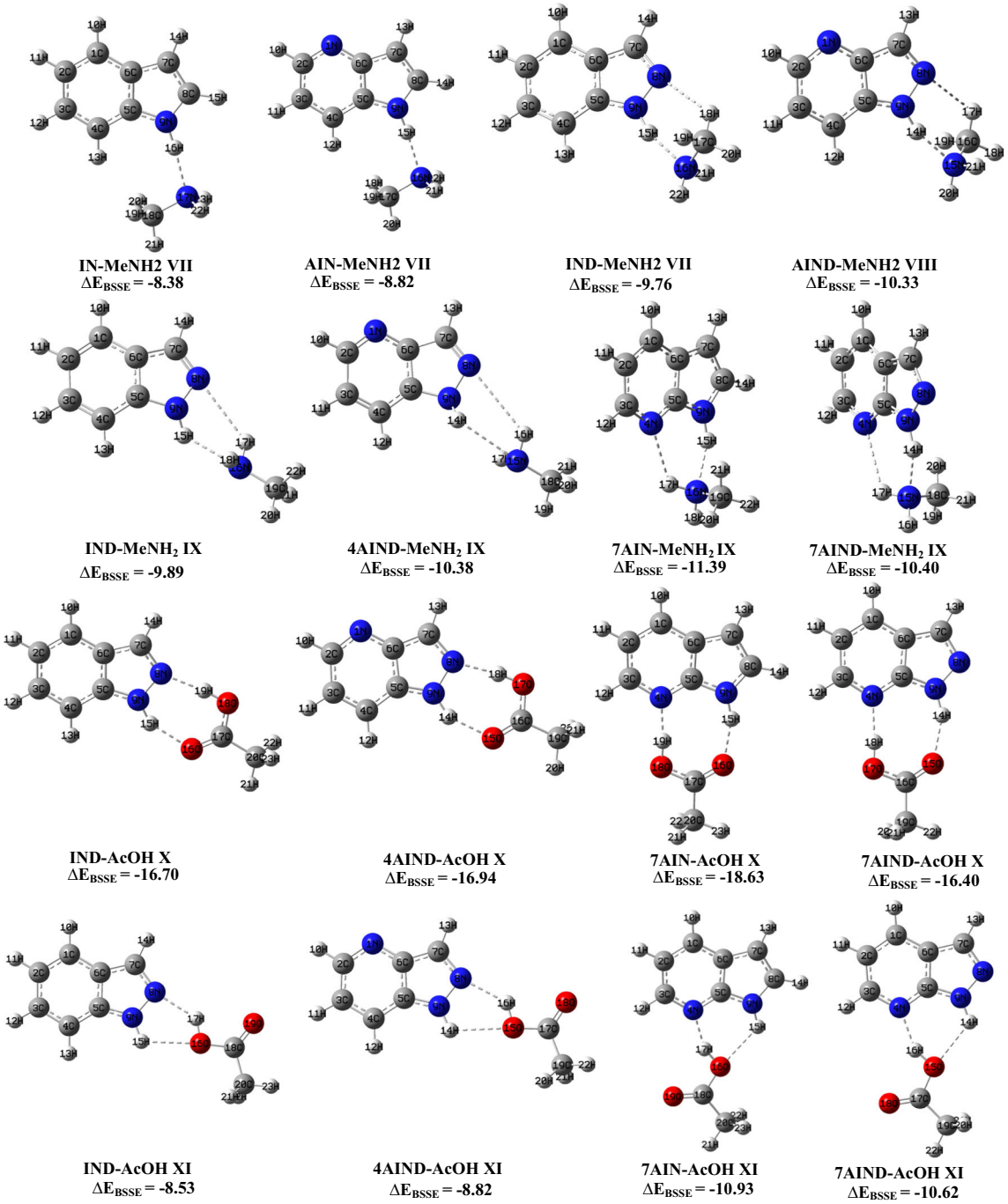

Fig. 2 (continued)

interaction, while for the $_{MeNH2}$N-H···N_{Indene}, it is 55° to 60°. The HBs of type N-H···N are expected to make a substantial contribution to protein structure and its stability and they are known to exist in nucleic acids. The stabilization energies of complexes of Indene analogs with $MeNH_2$ is 0.39–2.37 kcal/mol higher than that of their corresponding complexes with MeOH which reflect that $MeNH_2$ hydrogen bonds to Indene analogs more strongly than MeOH and this can be rationalized in terms of the fact that $MeNH_2$ is more basic than MeOH.

(D) Indene-AcOH complexes The hydroxyl group in AcOH can adopt a *cis* or *trans* orientation with respect to the carbonyl group. The more stable orientation having *cis* arrangement of C=O and O-H is selected for the present study and it leads to two distinct types of complexes **X** and **XI**. In the "**X**" set of complexes, AcOH hydrogen bonds to Indene analogs through different proton donor (OH) and acceptor (C=O) sites. In these complexes, C=O and O-H bonds of AcOH are hydrogen bonded to N-H and N_5/N_6 sites of Indene analogs respectively

Table 1 Hydrogen bond (HB) distances *r* (in Å) and angles θ (in °) of complexes of N-heterocyclic analogs of Indene with amino acid side-chain mimics at the MP2/aug-cc-pVDZ (L2) level; BSSE corrected stabilization energies (ΔE_{BSSE} in kcal/mol) at the wB97XD/aug-cc-pVDZ (L1) and MP2/aug-cc-pVDZ (L2) levels; change in bond length Δd (in Å); and shifts of stretching frequencies Δυ (in cm^{-1}) for the HB donor group (D-H) at the wB97XD/aug-cc-pVDZ (L1) level

	Complexes	HB distance *r* (Å)		HB angle θ (°)		Δd	Δυ	ΔE_{BSSE} (−ve)	
								L1	L2
MeOH	IN-MeOH I	O17···H16	1.962	N9-H16···O17	144.49	0.008	− 133.75	7.16	6.85
		N9···H19	2.750	C18- H19···N9	113.68	0.000	+ 15.97		
	4AIN-MeOH I	O16···H15	1.958	N9-H15···O16	143.68	0.009	− 135.38	7.43	7.12
		N9···H18	2.768	C17-H18···N9	112.85	0.000	+ 18.78		
	IND-MeOH II	O16···H15	1.866	N9-H15···O16	156.74	0.010	− 186.95	7.85	7.53
		N8···H20	2.752	C17-H20···N8	123.25	0.007	+ 21.35		
	4AIND-MeOH II	O15···H14	1.846	N9-H14···O15	158.45	0.012	− 194.51	8.10	7.96
		N8···H19	2.774	C16-H19···N8	122.01	0.004	+ 23.23		
	IND-MeOH III	O16···H15	2.097	N9-H15···O16	124.34	0.006	− 103.81	8.63	8.39
		N8···H17	2.104	O16-H17···N8	132.46	0.009	− 157.09		
	4AIND-MeOH III	O16···H14	2.053	N9-H14···O16	126.18	0.007	−109.27	9.10	8.79
		N8···H15	2.136	O16-H15···N8	130.29	0.011	− 145.28		
	7AIN-MeOH III	O16···H15	1.997	N9-H15···O16	135.33	0.010	− 160.90	11.52	11.00
		N4···H17	1.940	O16-H17···N4	150.07	0.017	− 305.89		
	7AIND-MeOH III	O15···H14	2.027	N9-H14···O15	131.21	0.008	− 129.66	10.61	10.00
		N4···H16	1.983	O15-H16···N4	148.00	0.014	− 251.31		
MeSH	IN-MeSH IV	S17···H16	2.585	N9-H16···S17	168.29	0.007	− 135.24	5.82	5.73
	AIN-MeSH IV	S16···H15	2.549	N9-H15···S16	170.21	0.009	− 138.29	6.02	5.84
	IND-MeSH V	S16···H15	2.535	N9-H15···S16	134.88	0.011	− 175.24	6.45	6.32
		N8···H18	2.686	C17-H18···N8	143.58	0.000	+ 21.96		
	4AIND-MeSH V	S15···H14	2.523	N9-H14···S15	136.94	0.013	− 189.23	6.62	6.57
		N8···H17	2.652	C16-H17···N8	141.29	0.000	+ 23.34		
	IND-MeSH VI	S16···H15	2.515	N9-H15···S16	135.63	0.006	− 110.25	6.68	6.59
		N8···H17	2.397	S16-H17···N8	131.81	0.002	− 17.89		
	4AIND-MeSH VI	S16···H14	2.505	N9-H14···S16	136.27	0.007	− 113.17	6.83	6.69
		N8···H15	2.390	S16-H15···N8	132.85	0.003	− 18.11		
	7AIN-MeSH VI	S16···H15	2.412	N9-H15···S16	134.28	0.009	− 145.29	7.32	7.12
		N4···H17	2.325	S16-H17···N4	132.89	0.005	− 40.60		
	7AIND-MeSH VI	S15···H14	2.448	N9-H14···S15	139.44	0.008	− 136.38	7.05	6.87
		N4···H16	2.385	S15-H16···N4	133.76	0.004	− 17.08		
$MeNH_2$	IN-$MeNH_2$ VII	N17···H16	1.926	N9-H16···N17	176.25	0.019	− 339.78	8.73	8.38
	4AIN-$MeNH_2$ VII	N16···H15	1.911	N9-H15···N16	175.76	0.020	− 350.49	9.14	8.82
	IND-$MeNH_2$ VIII	N16···H15	1.862	N9-H15···N16	160.53	0.022	− 380.83	10.07	9.76
		N8···H18	2.747	C17-H18···N8	124.37	−0.001	+ 18.16		
	4AIND-$MeNH_2$ VIII	N15···H14	1.847	N9-H14···N15	160.78	0.028	− 424.42	10.82	10.33
		N8···H17	2.748	C16-H17···N8	123.98	−0.001	+ 21.18		
	IND-$MeNH_2$ IX	N16···H15	1.925	N9-H15···N16	149.42	0.018	− 349.89	10.28	9.89
		N8···H17	2.656	N16-H17···N8	123.26	0.001	− 12.31		
	4AIND-$MeNH_2$ IX	N15···H14	1.901	N9-H14···N15	147.58	0.019	− 352.67	10.63	10.38
		N8···H16	2.623	N15-H16···N8	124.26	0.002	− 12.98		

Table 1 (continued)

	Complexes	HB distance r (Å)		HB angle θ (°)		Δd	Δυ	ΔE_{BSSE} (−ve)	
								L1	L2
	7AIN-$MeNH_2$ IX	N16···H15	1.891	N9-H15···N16	144.46	0.020	− 343.62	11.75	11.39
		N4···H17	2.564	N16-H17···N4	119.36	0.004	− 33.71		
	7AIND-$MeNH_2$ IX	N15···H14	1.899	N9-H14···N15	145.66	0.020	− 343.79	10.68	10.40
		N4···H17	2.405	N15-H17···N4	125.61	0.003	− 14.73		
AcOH	IND-AcOH X	O16···H15	1.847	N9-H15···O16	148.02	0.015	− 233.55	17.32	16.70
		N8···H19	1.738	O18-H19···N8	172.75	0.032	− 669.96		
	4AIND-AcOH X	O15···H14	1.824	N9-H14···O15	148.98	0.016	− 256.22	17.86	16.94
		N8···H18	1.744	O17-H18···N8	172.46	0.030	− 639.29		
	7AIN-AcOH X	O16···H15	1.828	N9-H15···O16	160.19	0.017	− 276.72	19.15	18.63
		N4···H19	1.692	O18-H19···N4	174.61	0.043	− 874.98		
	7AIND-AcOH X	O15···H14	1.860	N9-H14···O15	153.99	0.014	− 218.95	17.07	16.40
		N4···H18	1.735	O17-H18···N4	175.26	0.035	− 737.09		
	IND-AcOH XI	O16···H15	2.284	N9-H15···O16	124.26	0.002	− 48.29	8.85	8.53
		N8···H17	1.868	O16-H17···N8	153.24	0.020	− 310.29		
	4AIND-AcOH XI	O15···H14	2.272	N9-H14···O15	125.23	0.003	− 50.16	9.10	8.82
		N8···H16	1.852	O15-H16···N8	151.34	0.022	− 326.23		
	7AIN-AcOH XI	O16···H15	2.226	N9-H15···O16	126.63	0.005	− 54.18	11.32	10.93
		N4···H17	1.810	O16-H17···N4	154.98	0.027	− 489.93		
	7AIND-AcOH XI	O15···H14	2.250	N9-H14···O15	121.29	0.004	− 52.24	11.07	10.62
		N4···H16	1.828	O15-H16···N4	151.63	0.024	− 450.32		

($_{AcOH}$C=O···H-N_{Indene} and $_{Indene}$N···O-H_{AcOH}) leading to the formation of seven-membered cyclic ring structure in IND-AcOH **X** and 4AIND-AcOH **X** and eight-membered ring structure in 7AIN-AcOH **X** and 7AIND-AcOH **X** complexes. The complexes in which AcOH coordinates to Indene analogs solely through the hydroxyl group are marked as "**XI**." Indeed, in this configuration, AcOH binds to Indene analogs through N-H···O and N···H-O HBs. Likewise, similar HBs' interactions are also present in Indene-MeOH **III** complexes. On comparing Indene-AcOH **XI** and Indene-MeOH **III** complexes, it is interesting to note that N···H-O HB interaction is comparatively stronger whereas N-H···O HB interaction is weaker in former complexes with respect to latter complexes which can be justified in terms of the fact that the neighboring carbonyl group in the AcOH enhances the acidity of the hydroxyl group and reduces the basicity of oxygen of hydroxyl group. The "**X**" set of complexes has the higher stabilization energies, almost double in comparison with the "**XI**" set of complexes. The reason behind is that there is probability of resonance assisted hydrogen bonding (RAHB) mechanism in the "**X**" set of complexes which enhances the HB strength, thus supporting the relatively higher stability of these complexes. This is also supported by NBO analysis. Moreover, in the "**X**" set of complexes, the two HBs closely approach linearity in the seven/eight-membered ring resulting in strong HBs whereas the five-membered cyclic arrangement in case of "**XI**" set of complexes causes HBs being bent more, resulting in relatively weaker HBs.

Vibrational properties of hydrogen bond donor group

Table 1 reflects the variation in bond distances (Δd in Å) and shifts of stretching vibrational frequencies (Δ in cm^{-1}) of the HB donor group upon complex formation relative to monomers. In all the complexes under study, complex formation leads to red shift of conventional HB donors (N-H, O-H) and blue shift of unconventional HB donor (C-H). From the results of the vibrational analysis, it is observed that the lengthening of the HB donor is found in all red-shifting cases and the shrinking of HB donor is always associated with blue-shifted complexes. As anticipated for conventional HB donors, the O-H/N-H/S-H bonds of amino acid side-chain mimics and N-H bond of Indene analogs undergo red shifts when engaged in hydrogen bonding. The Δ values of O-H/N-H/S-H HB donors of amino acid side-chain mimics are found to follow the order $_{AcOH}$O-H (− 310.29 to − 874.98 cm^{-1}) > $_{MeOH}$O-H (− 145.28 to − 305.89 cm^{-1}) > $_{MeSH}$S-H (− 17.08 to − 40.60 cm^{-1}) > $_{MeNH2}$N-H (− 12.31 to − 33.71 cm^{-1}). Despite of having a similar type of hydrogen bonding interactions (O-H···N_{Indene} and O···H-N_{Indene}) in Indene-AcOH **XI** and Indene-MeOH **III** complexes, the red shift in the O-H stretching frequency of former complexes is found to be nearly two times higher than that of the latter complexes. The red shift stretching frequency of the N-H of Indene which occurred upon the complexation with amino acid side-chain mimics lay down in the order N-H···N_{MeNH2} (− 339.78 to − 424.42 cm^{-1}) > N-H···O=C_{AcOH} (− 218.95 to − 276.72 cm^{-1}) > N-H···O_{MeOH} (− 103.81 to − 194.51 cm^{-1}) > N-H···S_{MeSH} (− 110.25 to − 189.23 cm^{-1}). This is also supported from the proton affinity of acceptor atoms (O, N, S) of amino acid side-chain mimics that exactly lie in the same order $MeNH_2$ (214.7 kcal/mol) > AcOH (187.3 kcal/mol) > MeOH (180.2 kcal/mol) > MeSH (162.9 kcal/mol). This reflects that the abovementioned HB interactions obey acid-base formalism. There is good linear correlation observed in the red shifts in the vibrational stretching frequency of the N-H bond of indene analogs with the elongation of the N-H bond upon complex formation (shown in Fig. 3). It is noteworthy that the larger red shift of N-H which has been observed in the Indene-MeOH complexes in comparison with the Indene-H_2O as replacement of one of the hydrogens in the H_2O by methyl group increases the electron density on the oxygen due to the positive inductive effect of methyl group, which induces a stronger interaction between the oxygen of MeOH and acidic hydrogen of N-H of Indene analogs. Red shifts in the hydrogen-bonded N-H stretching frequencies in case of the Indene-MeSH complexes are found to be comparable with those of the Indene-MeOH complexes. This infers that N-H···S HBs in proteins and biomolecules are equally strong HBs as their oxygen counterpart. Hence, their significance cannot be neglected or overlooked in comparison with the N-H···O and N-H···O=C HBs in biomolecules.

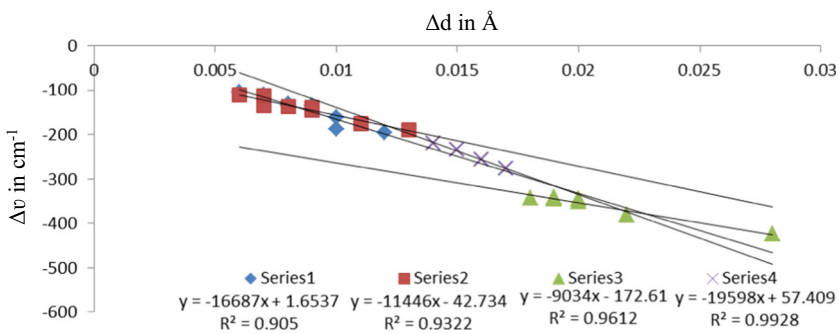

Fig. 3 Plot of shift in vibrational stretching frequency of N-H of Indene against elongation of N-H bond. The straight lines are least squares fit to the data points of N-H···O (diamond), N-H···S (squares), N-H···N (triangle), and N-H···O=C (cross) with R^2 values of 0.905, 0.932, 0.961, and 0.993 respectively

Natural bond orbital (NBO) analysis

Second-order delocalization energy [$E^{(2)}$]

NBO analysis has been carried out to investigate the donor-acceptor charge transfer delocalization interactions. These interactions can be derived from second-order perturbation energies $E^{(2)}$ enlisted in Table S4. It is observed that the $E^{(2)}$ values for $n_{N(MeNH2)} \rightarrow \sigma^*_{N\text{-}H(Indene)}$ orbital interactions in Indene-$MeNH_2$ complexes are significantly higher in comparison with $n_{O(MeOH)} \rightarrow \sigma^*_{N\text{-}H(Indene)}$ in Indene-MeOH complexes which can be rationalized on the basis of the fact that HB acceptor ability of $MeNH_2$ is better than that of MeOH. The $E^{(2)}$ values for $n_{N(MeNH2)} \rightarrow \sigma^*_{N\text{-}H(Indene)}$ orbital interactions are remarkably higher than that of the $n_{N(Indene)} \rightarrow \sigma^*_{N\text{-}H(MeNH2)}$ in Indene-$MeNH_2$ **IX** complexes which can be justified in terms of the fact that the nitrogen of $MeNH_2$ (sp^3 hybridized) is a better HB acceptor in comparison with the pyridinic nitrogen (sp^2 hybridized) atom of Indene analogs as increasing the s-character of nitrogen lone pair decreases the HB acceptor tendency ($sp^3 > sp^2$). The double hydrogen-bonded closed ring structured Indene-AcOH **X** complexes exhibit a remarkable resonance-assisted hydrogen bonding (RAHB) mechanism as a result of which there is a significant increase in $E^{(2)}$ values of $n_{O(AcOH)} \rightarrow \sigma^*_{N\text{-}H(Indene)}$ and $n_{N(Indene)} \rightarrow \sigma^*_{O\text{-}H(AcOH)}$ orbital interactions. It is interesting to note that $E^{(2)}$ values for $n_{N(Indene)} \rightarrow \sigma^*_{O\text{-}H(AcOH)}$ orbital interactions are nearly double than that of $n_{O(AcOH)} \rightarrow \sigma^*_{N\text{-}H(Indene)}$ in Indene-AcOH **X** complexes as σ^*(O-H) orbital of AcOH has better electron accepting tendency than σ^*(N-H) of indene analogs. In accord with this notion, there is a greater role of σ^*(O-H) hyperconjugative interaction in O-H bond lengthening of the AcOH in comparison with the σ^*(N-H) orbital of Indene analogs in the N-H bond. It is observed that there is enhancement in $E^{(2)}$ values of the $n_{O/S/N} \rightarrow \sigma^*_{N\text{-}H(Indene)}$ orbital interactions in IND/AIND-Z complexes relative to their corresponding IN/AIN-Z complexes which reflect that the presence of an additional nitrogen atom in the five-membered ring increases the electron accepting tendency of σ^* antibonding N-H orbitals that urge to the weakening and elongation of the N-H bond and is also harmonious with the concomitant increase in red shift stretching vibration of the bond. It is also noticed that the $E^{(2)}$ values for the $n_{O/N/S} \rightarrow \sigma^*_{N\text{-}H(Indene)}$ orbital interactions in the IN/IND-Z complexes are lower in comparison with their aza analogs AIN/AIND-Z which highlight the fact that the fusion of pyridine ring to single five-membered ring makes the pyrrolic nitrogen atom function as a better HB donor in comparison with the fusion of benzene ring. The discussion of charge transfer analysis is provided in Section S1.

Topological parameters

Atoms in molecules (AIM) theory has been performed on 1:1 Indene-Z complexes to investigate the topology of electron density and intermolecular hydrogen bond properties. The electron density ρ and its Laplacian $\nabla^2\rho$ at the bond critical points (BCPs) computed at the MP2/aug-cc-pVDZ level of theory for all the complexes are listed in Table S5; see Section S2 for detailed analysis. The ρ and $\nabla^2\rho$ values at the BCPs are found to lie in the range of 0.002–0.051 au and 0.021–0.141 au, respectively. These values of the ρ and $\nabla^2\rho$ values are well within the range specified for the existence of the HB. Moreover, ρ and $\nabla^2\rho$ values at the BCPs for all the complexes are in line with the computed stabilization energies (shown in Fig. S2 and S3). Comparison of relative values of ρ and its $\nabla^2\rho$ parameters for N-H···O versus N-H···S bound complexes suggests that hydrogen bonding interaction involving the sulfur center are weaker than those involving the oxygen center. These parameters also suggest that the electrostatic component of the hydrogen bonding interaction must be greater for the Indene-MeOH complexes relative to that of Indene-MeSH complexes. Larger values of ρ and $\nabla^2\rho$ have been observed for $_{Indene}$N-H···N_{MeNH2} HBs in comparison with $_{MeNH2}$N-H···N_{Indene} in Indene-$MeNH_2$ **IX** complexes, which corroborates that HB acceptor tendency strongly depends on hybridization of nitrogen atom [$MeNH_2$ (sp^3) and Indene (sp^2)] with the order $sp^3 > sp^2$. Increment in ρ and $\nabla^2\rho$ values for the N-H···Y (Y = O, S, N) HB interaction has been observed for IND/AIND-Z relative to that of IN/AIN-Z complexes which are consistent with the fact that incorporation of nitrogen atom in the five-membered ring boosts the HB donor tendency of ring nitrogen atom.

Summary and concluding remarks

The present work analyzed thirty-two hydrogen-bonded complexes comprised of N-heterocyclic analogs of Indene-Indole (**IN**), Indazole (**IND**), Azaindole (**AIN**), and Azaindazole (**AIND**) as one partner and amino acid side-chain mimics (**Z**), MeOH, MeSH, $MeNH_2$, and AcOH, as the other partner that have been optimized at the wB97XD/aug-cc-pVDZ and MP2/aug-cc-pVDZ levels. By analyzing the geometries, vibrational frequencies, natural bond orbitals, and stabilization energies, the following inferences can be made:

- The stabilization energies of hydrogen-bonded complexes of N-heterocyclic analogs of indene with amino acid side-chain mimics follow the order Indene-AcOH > Indene-$MeNH_2$ > Indene-MeOH > Indene-MeSH, which can be attributed to the fact that HB interaction ability of amino acid side-chain mimics follows the similar sequence AcOH > $MeNH_2$ > MeOH > MeSH.

- The HB donor ability of N-H bond of N-heterocyclic analogs of Indene towards amino acid side-chain mimics follow the sequence AIND > IND > AIN > IN. This sequence reflects that the introduction of nitrogen atom in the five-membered ring of indene analogs expedites the tendency of pyrrolic nitrogen atom to act as a better HB donor. This sequence also reflects that the fusion of the pyridine ring with the five-membered ring provides higher stabilization energies in comparison with the fusion of benzene ring as it is reflected from the higher stabilization energies of the AIN/AIND-Z complexes relative to that of the IN/IND-Z.
- Geometrical parameters indicate that the strength sequence of N-H···Y (Y = O, N, S) HBs from strongest to the weakest is N-H···O=C_{AcOH} > N-H···N_{MeNH2} > N-H···O_{MeOH} > N-H···S_{MeSH}. From this trend, it can be inferred that carbonyl oxygen of AcOH acts as better HB acceptor in comparison with hydroxyl oxygen of MeOH. On the other way, strengths of N···H-Y (Y = O, N, S) HBs lay down in the order $_{Indene}$N···H-O_{AcOH} > $_{Indene}$N···H-O_{MeOH} > $_{Indene}$N···H-S_{MeSH} > $_{Indene}$N···H-N_{MeNH2}. This order reflects that the hydroxyl group of AcOH acts as a better HB donor in comparison with MeOH.
- NBO analysis illustrates the effect of hybridization on HB acceptor strength of nitrogen by comparing the $E^{(2)}$ values of $n_{N(MeNH2)} \rightarrow \sigma^*_{N\text{-}H(Indene)}$ and $n_{N(Indene)} \rightarrow \sigma^*_{N\text{-}H(MeNH2)}$ orbital interactions in Indene-$MeNH_2$ **IX** complexes. The comparison clearly shows that $E^{(2)}$ values for $n_{N(MeNH2)} \rightarrow \sigma^*_{N\text{-}H(Indene)}$ orbital interaction is significantly higher in comparison with $n_{N(Indene)} \rightarrow \sigma^*_{N\text{-}H(MeNH2)}$ which is consistent with our general prediction that nitrogen of $MeNH_2$ (sp^3 hybridized) is a better HB acceptor in comparison with the pyridinic nitrogen atom of indene (sp^2 hybridized), and increased p-character in the nitrogen lone pair increases the HB acceptor strength ($sp^3 > sp^2$).

Computational details and choice of method

The geometry optimization of N-heterocyclic analogs of Indene and their parallel hydrogen-bonded complexes with amino acid side-chain mimics has been carried out at MP2/aug-cc-pVDZ and wB97XD/aug-cc-pVDZ levels. All the calculations of hydrogen-bonded complexes of N-heterocyclic analogs of Indene with amino acid side-chain mimics have been done by employing Gaussian 09 W package [26]. The stabilization energies of the complexes have been estimated at the abovementioned levels and are further corrected for basis set superposition error by employing counterpoise procedure. Frequency calculations have been performed at the wB97XD/aug-cc-pVDZ level to ensure that the obtained structures correspond to true energy minima [27]. The natural bond orbital analysis has been determined to obtain second-order delocalization energies, charge transfer, and atomic charges at the MP2/aug-cc-pVDZ level via the method incorporated in the Gaussian 09 W package [28]. The AIMALL program has been utilized to calculate the topological properties at bond critical points and ring critical points of the studied complexes at the MP2/aug-cc-pVDZ level [29].

Supporting information Hydrogen bond (HB) distances r (in Å) and angles θ (in °) of complexes of N-heterocyclic analogs of Indene with water at MP2/aug-cc-pVDZ (L2) level; BSSE corrected stabilization energies (ΔE_{BSSE} in kcal/mol) at the wB97XD/aug-cc-pVDZ (L1) and MP2/aug-cc-pVDZ (L2) levels; and change in bond length Δd (in Å) and shifts of stretching frequencies Δυ (in cm^{-1}) for the HB donor group (D-H) at the wB97XD/aug-cc-pVDZ (L1) level are listed in Table S1; second-order delocalization energies $E,^{(2)}$ atomic charges, and amount of charge transfer of Indene-H_2O complexes at the L2 level are displayed in Table S2; topological and energetic properties at the bond critical points (bcps) and the ring critical points (rcps) of Indene-H_2O complexes evaluated at the L2 theoretical level using AIM analysis are summarized in Table S3; second-order delocalization energies $E^{(2)}$ (in kcal/mol) associated with orbital interactions, atomic charges (in au), and amount of charge transfer from indene to amino acid side-chain mimics (CT in e) at the L2 level are summarized in Table S4; topological and energy properties at the bond critical points (BCPs) and the ring critical points (RCPs) for the complexes of N-heterocyclic analogs of Indene with amino acid side-chain mimics evaluated at the MP2/aug-cc-pVDZ theoretical level using AIM analysis (All the values are in au) are discussed in Table S5; optimized geometries of 1:1 hydrogen bonded complexes of Indene-H_2O complexes at the MP2/aug-cc-pVDZ level are shown in Fig. S1; correlation between stabilization energy (ΔE_{BSSE}) and ρ (au) at the MP2/aug-cc-pVDZ level is plotted in Fig. S2; correlation between stabilization energy (ΔE_{BSSE}) and $\nabla^2\rho$ (au) at the MP2/aug-cc-pVDZ level is plotted in Fig. S3; discussion of charge transfer analysis and AIM analysis is given in Sections S1 and S2, respectively; Tables S6–S18 include the optimized parameters for the complexes of N-heterocyclic analogs of Indene with water/amino acid side-chain mimics at the wB97XD/aug-cc-pVDZ (L1) and MP2/aug-cc-pVDZ (L2) levels.

Funding information The authors are highly thankful to UGC (University Grants Commission) New Delhi, India, for the financial assistance.

References

1. Muller-Dethlefs K, Hobza P (2010) Non-covalent interactions: theory and experimentIst edn. Cambridge, RSC, pp 1–238
2. Muller-Dethlefs K, Hobza P (2000) Noncovalent interactions: a challenge for experiment and theory. Chem Rev 100:143–167
3. Kyungsun K, Friesner RA (1997) Hydrogen bonding between amino acid backbone and side chain analogues: a high-level ab initio study. J Am Chem Soc 119:12952–12961
4. Nagy PI, Erhardt PW (2006) Ab initio study of hydrogen-bond formation between cyclic ethers and selected amino acid side chains. J Phys Chem A 110:13923–13932
5. Huang N, MacKerell Jr AD (2002) An ab initio quantum mechanical study of hydrogen-bonded complexes of biological interest. J Phys Chem A 106:7820–7827
6. Cheng AC, Frankel AD (2004) Ab initio interaction energies of hydrogen-bonded amino acid side chain-nucleic acid base interactions. J Am Chem Soc 126:434–435

7. Czyznikowska Z, Lipkowski P, Gora RW, Zalesny R, Cheng AC (2009) On the nature of intermolecular interactions in nucleic acid base-amino acid side-chain complexes. J Phys Chem B 113:11511–11520
8. Nagy PI, Erhardt PW (2008) Ab initio study of hydrogen-bond formation between aliphatic and phenolic hydroxy groups and selected amino acid side chains. J Phys Chem A 112:4342–4354
9. Fang H, Kim Y (2011) Excited-state tautomerization in the 7-Azaindole-$(H2O)_n$ (n = 1 and 2) Complexes in the Gas Phase and in Solution: A Theoretical Study. J Chem Theory Comput 7:642–657
10. Fang H, Kim Y (2011) Theoretical studies for excited-state tautomerization in the 7-Azaindole-$(CH3OH)_n$ (n = 1 and 2) complexes in the gas phase. J Phys Chem A 115:13743–13752
11. Chopra N, Kaur D, Chopra G (2018) Nature and hierarchy of hydrogen-bonding interactions in binary complexes of azoles with water and hydrogen peroxide. ACS Omega 3:12688–12702
12. Chopra N, Kaur D, Chopra G (2018) Hydrogen bonded complexes of oxazole family: electronic structure, stability, and reactivity aspects. Struct Chem 29:341–357
13. Chopra N, Chopra G, Kaur D (2019) Exploring the role of consecutive addition of nitrogen atoms on stability and reactivity of hydrogen-bonded azine-water complexes. ACS Omega 4:8112–8121
14. Bhattacherjee A, Wategaonkar S (2017) Nature and hierarchy of noncovalent interactions in gas-phase binary complexes of indole and benzimidazole with ethers. J Phys Chem A 121:8815–8824
15. Kaushik NK, Kaushik N, Attri P, Kumar N, Kim CH, Verma AK, Choi EH (2013) Biomedical Importance of Indoles. Molecules 18:6620–6662
16. Lalit K, Shashi B, Kamal J (2012) The diverse pharmacological importance of indole derivatives: a review. IJRPS. 2(2):23–33
17. Zhang S-G, Liang C-G, Zhang W-H (2018) Recent advances in indazole-containing derivatives: synthesis and biological perspectives. Molecules. 23:2783
18. Gaikwad DD, Chapolikar AD, Devkate CG, Warad KD, Tayade AP, Pawar RP, Domb AJ (2015) Synthesis of indazole motifs and their medicinal importance: an overview. Eur J Med Chem 90:707–731
19. Dong JY, Zhang QJ, Wang ZT, Huang G, Li SS (2018) Recent advances in the development of indazole based anticancer agents. Chem Med Chem 13:1490–1507
20. Biswal HS, Wategaonkar S (2009) Nature of the N-H…S hydrogen bond. *J Phys Chem A 113*:12763–12773
21. Biswal HS, Gloaguen E, Loquais Y, Tardivel B, Mons M (2012) Strength of NH…S hydrogen bonds in methionine residues revealed by gas-phase IR/UV spectroscopy. J Phys Chem Lett 3(6):755–759
22. Mundlapati VR, Ghosh S, Bhattacherjee A, Tiwari P, Biswal HS (2015) Critical assessment of the strength of hydrogen bonds between the sulfur atom of methionine/cysteine and backbone amides in proteins. J Phys Chem Lett 6:1385–1389
23. Martsinovich N, Kantorovich L (2008) Comparative theoretical study of O- and S-containing hydrogen-bonded supramolecular structures. J Phys Chem C 112:17340–17350
24. Ueyama N, Nishikawa N, Yamada Y, Okamura T, Nakamura A (1996) Cytochrome P-450 model (Porphinato)(thiolato)iron(III) complexes with single and double N-H···S hydrogen bonds at the thiolate site. J Am Chem Soc 118:12826–12827
25. Ueyama N, Nishikawa N, Yamada Y, Okamura T, Oka S, Sakurai H, Nakamura A (1998) Synthesis and properties of octaethylporphinato(arenethiolato)iron(III) complexes with intramolecular N-H···S hydrogen bond: chemical function of the hydrogen bond. Inorg Chem 37:2415–2421
26. Frisch, M. J.; Trucks, G. W.; Schlegel, H. B.; Scuseria, G.E.; Robb, M. A.; Cheeseman, J. R.; Scalmani, G.; Barone, V.; Mennucci, B.; Petersson, G. A.; Nakatsuji, H.; Caricato, M.; Li, X.; Hratchian, H. P.; Izmaylov, A. F.; Bloino, J.; Zheng, G.; Sonnenberg, J. L.; Hada, M.; Ehara, M.; Toyota, K.; Fukuda, R.; Hasegawa, J.; Ishida, M.; Nakajima, T.; Honda, Y.; Kitao, O.; Nakai, H.; Vreven, T.; Montgomery, J. A.; Peralta, J. E.; Ogliaro, F.; Bearpark, M.; Heyd, J. J.; Brothers, E.; Kudin, K. N.; Staroverov, V. N.; Kobayashi, R.; Normand, J.; Raghavachari, K.; Rendell, A.; Burant, J. C.; Iyengar, S. S.; Tomasi, J.; Cossi, M.; Rega, N.; Millam, J. M.; Klene, M.; Knox, J. E.; Cross, J. B.; Bakken, V.; Adamo, C.; Jaramillo, J.; Gomperts, R.; Stratmann, R. E.; Yazyev, O.; Austin A. J.; Cammi, R.; Pomelli, C.; Ochterski, J. W.; Martin, R. L.; Morokuma, K.; Zakrzewski, V. G.; Voth, G. A; Salvador, P.; Dannenberg, J. J.; Dapprich, S.; Daniels, A. D.; Farkas, O.; Foresman, J. B.; Ortiz, J. V.; Cioslowski, J.; Fox, D. J. Gaussian 09, Revision B01. Wallingford CT, Gaussian, Inc. 2009
27. Boys SF, Moran D, Radom L (2007) An evaluation of harmonic vibrational frequency scale factors. J Phys Chem A 111:11683–11700
28. Reed AE, Curtiss LA, Weinhold F (1988) Intermolecular interactions from a natural bond orbital, donor-acceptor viewpoint. Chem Rev 88:899
29. Bader RFW (1990) Atoms in molecules - a quantum theory. Oxford University Press, Oxford